NJC

ROYAL SOCIETY OF CHEMISTRY

PAPER

View Article Online
View Journal | View Issue

Cite this: *New J. Chem.*, 2023, **47**, 2090

Electronic properties and supramolecular study of selenoureas with fluorinated-NHC ligands derived from imidazo[1,5-*a*]pyridines†

Luis Ángel Turcio-García,[a] Hugo Valdés,[b]* Antonino Arenaza-Corona,[a] Simón Hernández-Ortega[a] and David Morales-Morales[a]*

Received 23rd September 2022,
Accepted 6th December 2022

DOI: 10.1039/d2nj04699g

rsc.li/njc

A series of twelve selenourea compounds with fluorinated fragments were synthesized and characterized. The influence of fluorine atoms in the chemical shift of the ^{77}Se NMR was studied. The more fluorine atoms in the structure produced a downfield shift of the ^{77}Se signal, indicating a higher π-acidity character in the N-heterocycle. The relative position of the fluorine atom also affects the chemical shift of the ^{77}Se. It can be seen that a fluorine atom at 3-position, following by 4- and 2-position, respectively, produced a higher downfield shift. Interestingly, the opposite effect was observed for the $-CF_3$ group. The crystal structure of six selenourea compounds revelead that the predominant interactions were three: Se···H, F···F and F···H. The latter was corroborated by Hirshfeld surface analysis and 2D dimensional fingerprint plots of each crystal structure.

1. Introduction

The study of the electronic properties of N-heterocyclic carbene (NHC) ligands has helped to design new catalysts and advanced materials in a comprehensive way, since they are strongly related with the chemical properties of their organometallic derivatives.[1–10] The electronic properties can be quantified experimentally using infrared, pk_a measurements, cyclic voltammetry and NMR.[11–14] Infrared studies are by far the best known, and allow to determine the Tolman Electronic Parameter (TEP), which is related with the ν(CO) of carbonyl compounds based on Ni(0), Ir(I) and Rh(I).[15–18] In all cases, the TEP considers that the C–O bond in such complexes is weakened by d → π_{CO}* back-bonding, and thus the ν(CO) frequency correlates with how electron-rich the metal center is. However, in order to make a good correlation between ligands, their degree of π-accepting abilities must be similar.

Traditionally, the contribution of the π-accepting abilities of the NHC ligands has been negligible, considering that they are purely σ-donors, but there are some reports that confirm the π-accepting character of NHC ligands, being an important contribution to their electronic donor properties.[19,20] Thus, nowadays, both factors have to be considered. Experimentally, the π-acceptor strength of NHC ligands can be determined by ^{77}Se NMR studies.[21–24] Ganter and coworkers described that as the NHC π-acceptor strength character increases, the signal in the ^{77}Se NMR spectra shifts to downfield.[21] This approach may result suitable since the observable values covers a wide range of almost 800 ppm, thus, slightly variation in the π-acceptor strength produced by small structural changes can be detected. Furthermore, the selenourea compounds can be easily prepared from azolium salts, which are the same precursors for the synthesis of NHC complexes.

In a previous report, Jamil and Endot studied the influence of fluorine atoms in a series of Se–NHC compounds.[24] In this study, they compared the ^{77}Se NMR chemical shift of six symmetrical Se-imidazolylidene compounds, finding that the fluorine atoms produced a downfield shift. Murai and Shibahara observed a similar behavior for imidazo[1,5-*a*]pyridine-3-ylidenes derivatives,[23] while Hong and Chung determined the catalytic and electronic effect of a fluorine atom in the pyridine ring of a series of imidazo[1,5-*a*]pyridine compounds.[25] It is worth to note that fluorine atoms played an important role for the design of catalysts and pharmaceuticals, contributing to enhance their activities.[6,26,27] In this sense, fluorine atoms exhibited different roles, for example they form intramolecular M···F interactions, which produce more active catalysts.[25,28] Recently, we have reported that the catalytic activity of Rh(I) complexes with fluorinated NHC ligands derived from

[a] *Instituto de Química, Universidad Nacional Autónoma de México, Circuito Exterior, Ciudad Universitaria, Ciudad de México, C.P. 04510, Mexico. E-mail: damor@unam.mx*
[b] *Institut de Química Computacional i Catàlisi, Departament de Química, Universitat de Girona, c/Ma Aurèlia Capmany 69, Girona 17003, Spain. E-mail: hugo.valdes@udg.edu*

† Electronic supplementary information (ESI) available. CCDC 2194857–2194862. For ESI and crystallographic data in CIF or other electronic format see DOI: https://doi.org/10.1039/d2nj04699g

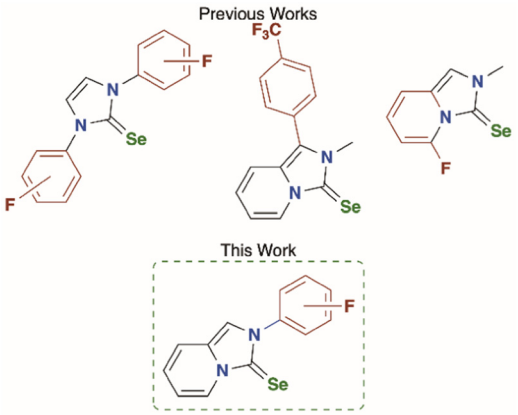

Fig. 1 Selected examples of fluorinated Se–NHC compounds.

imidazo[1,5-*a*]pyridine is strongly related with the number of fluorine atoms present on their structures; the more fluorine atoms are attached to the NHC ligand, the more active the related complex becomes.[29] Also, fluorine atoms can tune some important properties of organic compounds such as acidity, conformation or lipophilicity. The latter are key properties for the design of pharmaceuticals. Another important role of fluorine atoms is their relation to supramolecular structures.[30–32] The presence of fluorine may promote π–π interactions, hydrogen and halogen bonding,[33–36] allowing the design and synthesis of crystals with functional properties.

Based on the abovementioned, we decided to study the effect of fluorine atoms attached to the N-substituent of Se–NHC compounds derived from imidazo[1,5-*a*]pyridines (Fig. 1).[29,37] Furthermore, we studied the supramolecular interactions of six selenourea compounds by Hirshfeld surface analysis and 2D dimensional fingerprint plots.

2. Results and discussion

2.1 Synthesis and characterization of selenourea compounds

The selenourea compounds were synthesized by deprotonation of the corresponding imidazo[1,5-*a*]pyridium salt with NaH in THF at room temperature, following by the addition of Se^0 (Scheme 1). The desired compounds were obtained in good yields. The ^1H NMR spectra of these adducts showed the absence of the signal due to the NCHN fragment of the azolium, being the first evidence that the selenoureas were formed. In the $^{13}C\{^1H\}$ NMR spectra, the characteristic signal of the C═Se was found between 147 and 150 ppm. The latter values are similar to those described in the literature for related compounds.[23] The mass spectra of the selenoureas showed the molecular ion $[M]^+$ in all cases.

We also recorded the ^{77}Se NMR spectra of the selenoureas in $CDCl_3$ at 25.0 °C. The signals of the selenourea compounds with more fluorine atoms was shifted to downfield, indicating an increasing π-acidity of the NHC ligand (Fig. 2). The chemical shift of the signal is influenced by the position of the fluorine atom in the *N*-aryl substituent. When the fluorine atom is at

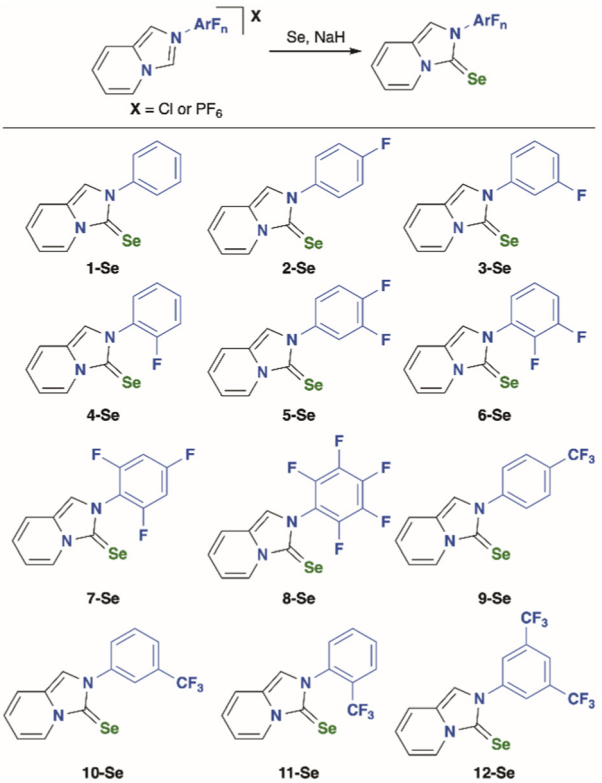

Scheme 1 Synthesis of the selenourea compounds.

2-position the chemical shift was 9.3 ppm, while at 4- and 3-position the signal was shifted to downfield, appearing at 9.5 and 14.7 ppm, respectively. However, when the substituent was a $-CF_3$ fragment the opposite effect was observed; the signal of the 2-substituent derivate was further downfield, in comparison with the 4- and 3-isomer. A similar behavior was observed for related compounds (Fig. 2). For example, the $\Delta^{77}Se$ for compounds I and II is 7.6 ppm, while the $\Delta^{77}Se$ for **1-Se** and **9-Se** is 10.7 ppm. This is a strong indication that the *N*-substituent produces a higher impact in the π-acidity than the substituent attached directly to the carbon of the heterocycle.

2.2 X-Ray and supramolecular analysis of six selenourea compounds

The molecular structures of six selenourea compounds, namely **3-Se** (CCDC 2194862), **4-Se** (CCDC 2194861), **7-Se** (CCDC 2194860), **9-Se** (CCDC 2194859), **11-Se** (CCDC 2194858) and **12-Se** (CCDC 2194857), were unambiguously determined by X-ray diffraction studies (Fig. 3). The suitable crystals were obtained by slow diffusion of hexane into a concentrated solution of the corresponding compound in dicholoromethane. Full crystal structure data can be found in the ESI.† The C–Se bond lengths were very similar in all compounds (~1.83 Å) and no correlation with the numbers of fluorine substituents was found.

A more detailed study of the X-ray molecular structures revealed that the angle between the imidazopyridineselenone and the fluorinated-phenyl ring, goes from 47° to 83.45°

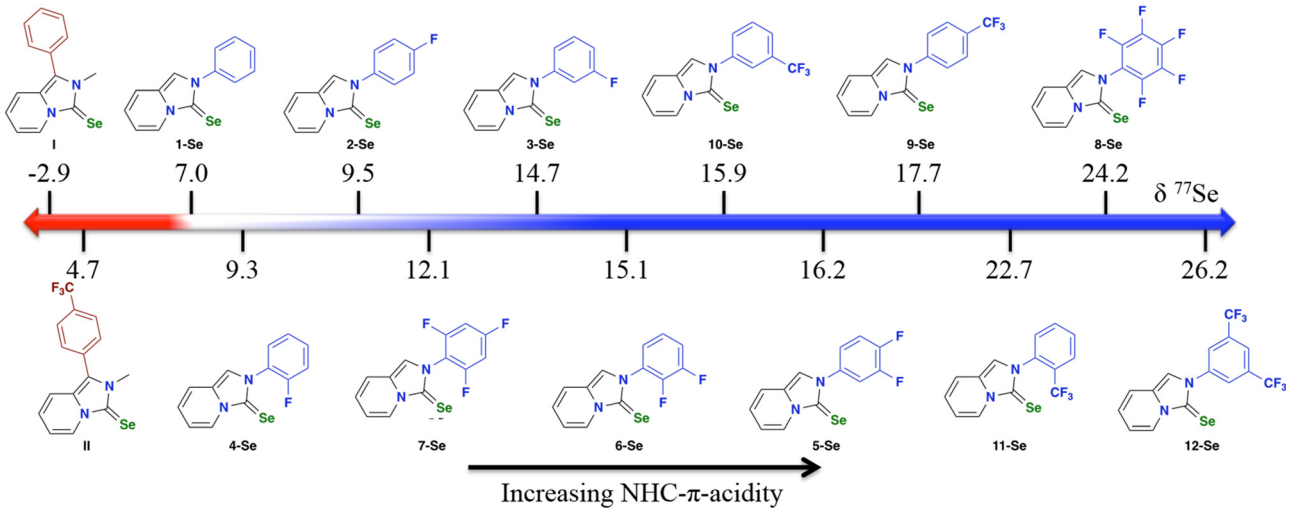

Fig. 2 ^{77}Se chemical shift for the selenourea compounds.

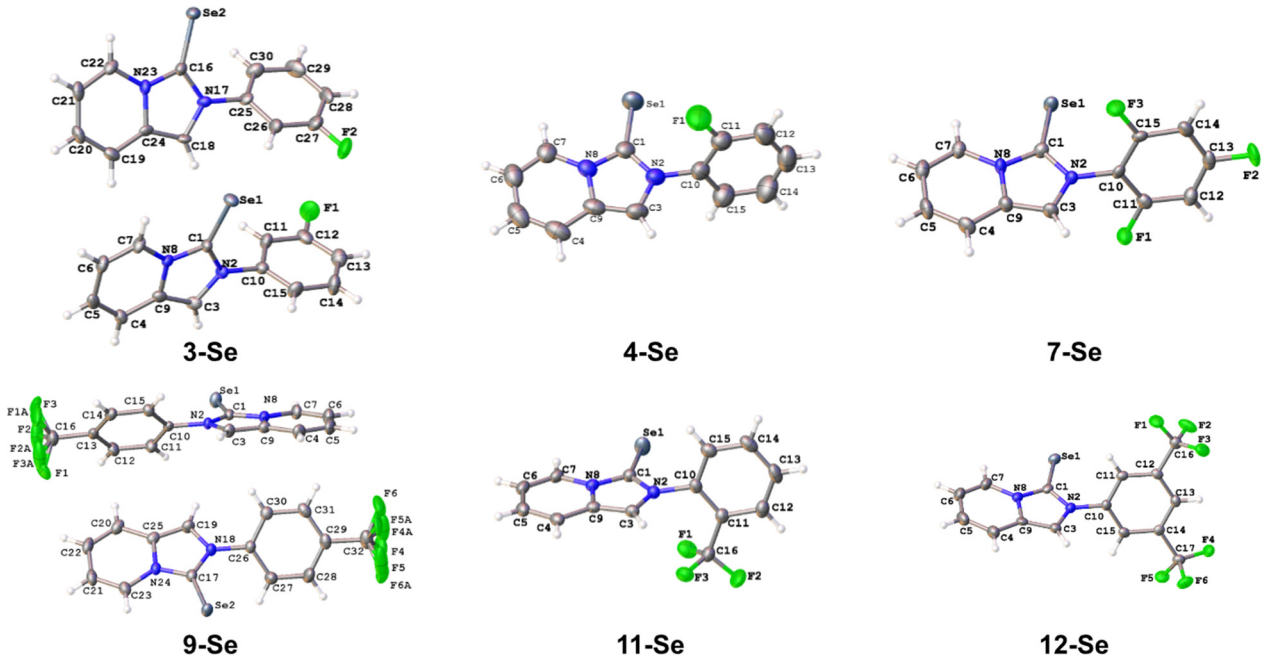

Fig. 3 Molecular structures of **3-Se**, **4-Se**, **7-Se**, **9-Se**, **11-Se** and **12-Se**. The ellipsoids are represented at 35% probability and hydrogen atoms were omitted for clarity. Selected bond length (Å): **3-Se** = Se(1)–C(1) 1.842(10), N(2)–C(1) 1.344(12), N(8)–C(1) 1.376(12), Se(2)–C(16) 1.842(10), N(23)–C(16) 1.364(12), N(17)–C(16) 1.371(12). **4-Se** = Se(1)–C(1) 1.828(3), N(2)–C(1) 1.361(3), N(8)–C(1) 1.367(3). **7-Se** = Se(1)–C(1) 1.833(7), N(2)–C(1) 1.355(9), N(8)–C(1) 1.366(9). **9-Se** = Se(1)–C(1) 1.832(2), N(8)–C(1) 1.367(3), N(2)–C(1) 1.367(3), Se(2)–C(17) 1.833(2), N(18)–C(17) 1.363(3), N(24)–C(17) 1.370(3). **11-Se** = Se(1)–C(1) 1.835(2), N(2)–C(1) 1.361(3), N(8)–C(1) 1.363(3). **12-Se** = Se(1)–C(1) 1.841(4), N(2)–C(1) 1.362(4), N(8)–C(1) 1.366(4). Selected bond angles (°): **3-Se** = N(2)–C(1)–N(8) 105.0(8), N(2)–C(1)–Se(1) 129.2(7), N(8)–C(1)–Se(1) 125.8(7), N(23)–C(16)–N(17) 103.9(8), N(23)–C(16)–Se(2) 125.3(7), N(17)–C(16)–Se(2) 130.7(8). **4-Se** = N(2)–C(1)–N(8) 104.3(2), N(2)–C(1)–Se(1) 128.8(2), N(8)–C(1)–Se(1) 126.85(19). **7-Se** = N(2)–C(1)–N(8) 111.9(6), N(2)–C(1)–Se(1) 129.0(5), N(8)–C(1)–Se(1) 126.2(5). **9-Se** = N(2)–C(1)–N(8) 104.1(2), N(8)–C(1)–Se(1) 125.96(18), N(2)–C(1)–Se(1) 129.81(17), N(18)–C(17)–N(24) 104.4(2), N(18)–C(17)–Se(2) 130.07(18), N(24)–C(17)–Se(2) 125.38(18). **11-Se** = N(2)–C(1)–N(8) 104.56(17), N(2)–C(1)–Se(1) 129.11(16), N(8)–C(1)–Se(1) 126.33(15). **12-Se** = N(2)–C(1)–N(8) 104.3(3), N(2)–C(1)–Se(1) 128.7(3), N(8)–C(1)–Se(1) 127.0(3).

(Fig. S1–S6, ESI†). The presence of F atoms or a CF_3 group at the *orto*- or *meta*-position produced a larger angle in comparison when a CF_3 is at *para*-position. The supramolecular structure of the selenoureas is mainly held by three non-covalent interactions: Se···H, F···F and F···H (Fig. 4). As can be seen in Table 1 the lengths of the non-covalent interactions are minor to the sum of van der Waals radii. Those compounds with a fluorinated functionality at the *ortho* position presented a Se···H interaction forming a chain along one axis, in addition, compound **11-Se** showed a head–tail π···π and a CH···F interaction.

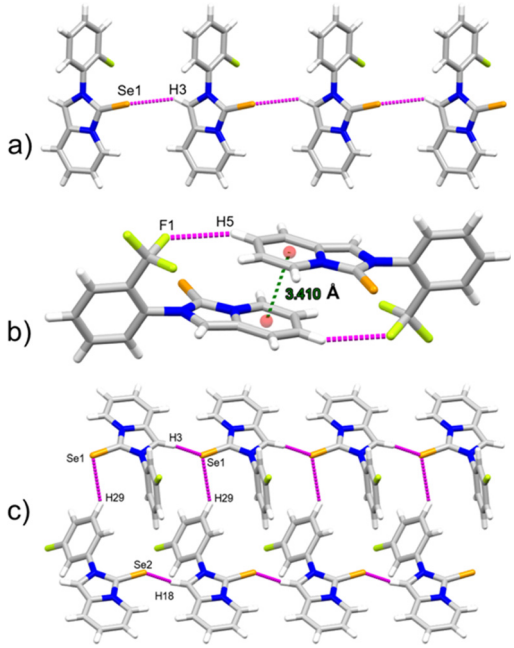

Fig. 4 Supramolecular arrangements (a) Chain formed through Se···H interaction in compound **4-Se**, (b) π···π and CH···π interactions in compound **11-Se** and (c) Se···H and bifurcate H···S···H interactions in compound **3-Se**.

The distance of the Cg···Cg was 3.410 Å and the CH···F was 2.644 Å. In contrast, when the fluorinated functionality is at the *meta* position, we found a bifurcate H···S···H interaction. Furthermore, compounds **7-Se** and **12-Se** showed a F···F bond interaction, with lengths going from 2.769 to 2.870 Å and an angle of ∼155°. These values are similar to those reported in the literature.[38–40] The C–H···F interactions that displayed compound **12-Se**, allowed the formation of 2D arrangements.

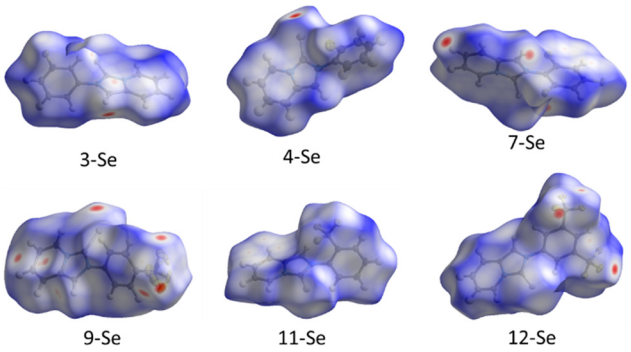

Fig. 5 Hirshfeld surface mapped over d_{norm} of compounds **3-Se**, **4-Se**, **7-Se**, **9-Se**, **11-Se** and **12-Se**.

2.3 Hirshfeld surface analysis

The proposed short interactions in the molecular structures of the selenourea compounds were studied by the Hirshfeld analysis, which helps to distinguish between strong and weak interactions. In the Hirshfeld analysis the surface of a certain molecule is constructed by allocating the space within a crystal structure into regions, providing information about intermolecular interactions in the crystal as the surface is determined by both the enclosed molecule and its closest neighbours.[41] In addition, we determined the two-dimensional fingerprint plots derived from Hirshfeld surface, to quantify the similarities and differences between the molecular crystal structures of the selenourea compounds.[42] To perform both analysis we employed CrystalExplorer software.[43]

The Hirshfeld surfaces mapped over d_{nom} of compounds **3-Se**, **4-Se**, **7-Se**, **9-Se**, **11-Se** and **12-Se** were determined. Fig. 5 shows the Hirshfeld surface of these compounds, as expected the red regions, which are due to the shorter interactions, were localized on the surface, and are due to the F···H/H···F,

Table 1 Principal interactions in the molecular structures of selenourea compounds

Compound	Interaction	Length (Å) D–X···A	Length (Å) D···A	Angle (°) D–X···A	Symmetry operation
3-Se	Se2–H18C18	2.878	3.509	124.91	$1 + x, y, z$
	Se1–H3C3	2.804	3.504	131.22	$-1 + x, y, z$
	Se1–H29C29	3.001	3.783	140.55	$-x, 1/2 + y, -z$
4-Se	Se1–H3C3	2.855	3.595	137.40	$x, -1 + y, z$
7-Se	Se1-H3C3	2.946	3.739	141.80	$-1 + x, y, z$
	Se1–H12C12	3.046	3.870	145.97	$-x, -y, 1 - z$
	Se1–H14C14	2.973	3.880	160.13	$-x, 1-y, 1 - z$
9-Se	F4-H19C19	2.552	3.129	119.31	$-1 + x, y, z$
	Se2–H5C5	3.041	3.934	157.51	$1-x, 1-y, 1 - z$
	Cg^3–H12C12	2.759	3.539	139.80	$-x, 1-y, 1 - z$
11-Se	Cg^1–H4C4	3.494	4.064	122.28	$-x, 1 - y, 1-z$
	Cg^2–H3C3	3.476	3.974	113.83	$-x, 1 - y, 1-z$
	F1–H5C5	2.664	3.544	154.24	$x, -1 + y, z$
12-Se	F2′–F2C16	2.769	4.017	155.51	$1-x, -y, 1 - z$
	Cg^4-F5C17	3.128	3.812	110.45	$-1 + x, y, z$
	F5–H7C7	2.460	3.154	129.80	$1/2 - x, 1/2 + y, 1/2 - z$
	Se1–H3C3	2.968	3.776	143.69	$1.5 - x, -1/2 + y, 1/2 - z$
	F4′–F4C17	2.870	3.401	101.54	$1.5 + x, 1.5 - y, -1/2 + z$

Cg^1: C1, N2, C3, N8, C9; Cg^2: C4, C5, C6, C7, N8, C9; Cg^3: C20, C21, C22, C23, N24, C25; Cg^4: C10, C11, C12, C13, C14, C15.

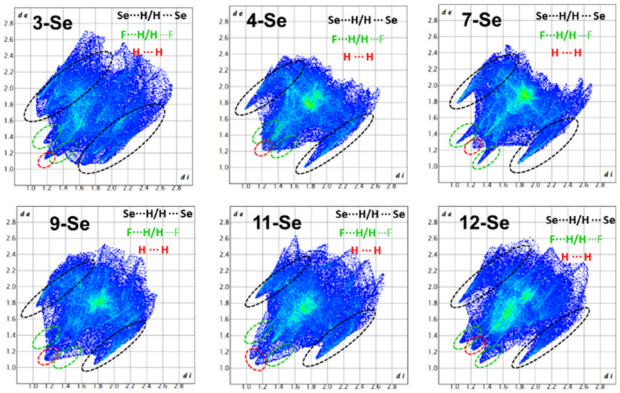

Fig. 6 2D dimensional fingerprint map showing all the contacts in the selenourea compounds.

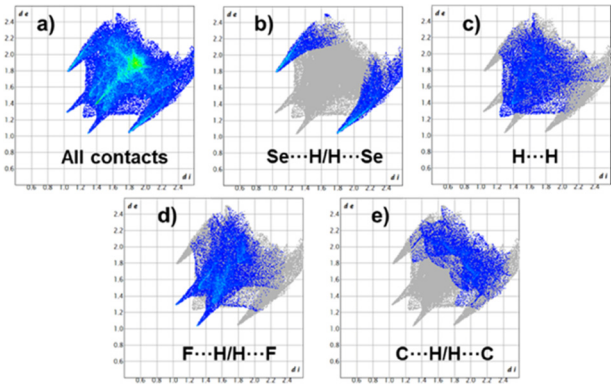

Fig. 7 Decomposed fingerprint plots for compound **7-Se**. (a) Represent all contacts (100%), (b) Se···H/H···Se is 15.1%, (c) H···H is 19.6%, (d) F···H/H···F is 25.5 and (e) C···H/H···C is 13.4%.

Se···H/H···Se, and other intermolecular interactions such as C···C, F···F, H···H and H···C/C···H.

Then, we calculated the 2D fingerprint plots of the Hirshfeld surfaces of six selenourea compounds **3-Se**, **4-Se**, **7-Se**, **9-Se**, **11-Se** and **12-Se** (Fig. 6). Despite the different relative position and number of the fluorine functionality in each selenourea compound, their plots showed some similar features. The most characteristic is the 'wings' at top left and bottom right of each plot, which is identified as result of the Se···H interaction (black dotted line, Fig. 6). Also, three 'peaks' in the bottom left of each plot are observed, and are consistent with the F···H and H···H interactions. The decomposed plot of the selenourea compounds provided further information about the percentage that contribute each non-covalent interaction. Chart 1 shows the calculated percentages and Fig. 7 the decomposed fingerprint of compound **7-Se** (in the ESI† there is the decomposed fingerprint of the rest of selenourea compounds).

In compound **7-Se**, the F···H interaction represents 25.5%, followed by the H···H interaction with 19.6% and Se···H interaction with 15.1%. Interestingly, in compounds **3-Se** and **4-Se**, where the fluorine atom is at *ortho* or *meta* position, the F···F interaction was scarcely or null observed. Similarly, the F···F interaction poorly contributed to compound **7-Se** (5.1%), **9-Se** (3.2%) and **11-Se** (5.3%), while in compound **12-Se** its contribution reached up to 13.8%. The Se···H interaction contributed to all compounds, going from 19.2% to 12.8%.

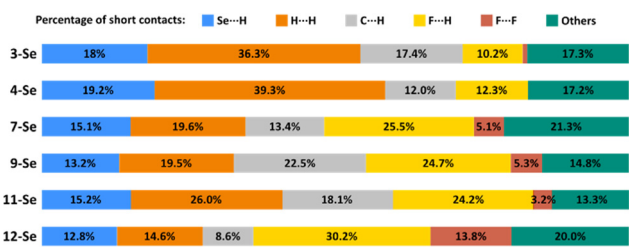

Chart 1 Plot of percentages of contacts observed in the selenourea compounds.

3. Conclusions

In conclusion, twelve new selenourea compounds were synthesized and fully characterized. We determined the molecular structure of 6 compounds. The influence of the fluorine atoms was not significant in the C–Se length. However, in the ^{77}Se NMR of the compounds we observed a clearly effect due to the presence of the fluorine atoms. Increasing the number of fluorine atoms produces a higher π-acidity of the N-heterocycle. Interestingly, an opposite effect was recorded in the ^{77}Se chemical shift due to the position of the fluorine atoms and $-CF_3$ fragments. The Hirshfeld surface analysis and their related 2D fingerprint plots of the six selenourea compounds with fluorinated functionalities were studied, revealing three main non-covalent interactions: Se···H, F···H and F···F. In the case of compounds 4-Se and 12-Se the increasing percentages of F···F contacts were proportional to the increasing of π-acidity of the N-heterocycle. The Se···H/H···Se and F···H/H···F intermolecular interaction appear as two conspicuous spikes in the 2D fingerprint plots.

Author contributions

L. A. T.-G. performed all the experiments. All authors discussed the results and wrote the manuscript.

Conflicts of interest

The authors declare that they have no known competing financial interests or personal relationship that could have appeared to influence the work reported in this paper.

Acknowledgements

We would like to thank Dr Francisco Javier Pérez Flores, Q. Eréndira García Ríos, MSc Lucia del Carmen Márquez Alonso, MSc Lucero Ríos Ruiz, Q. María de la Paz Orta Pérez, Q. Roció Patiño-Maya, Dr Beatriz Quiroz García and Dr Nuria Esturau Escofet for technical assistance. L. A. T.-G. would like

to thank Programa de Becas CONACYT (Número de becario: 626610). H. V. thanks CONACYT (CVU: 410706) and Generalitat de Catalunya (Beatriu de Pinós MSCA-Cofund 2019-BP-0080). The financial support of this research by PAPIIT-DGAPA-UNAM (PAPIIT IN210520) and CONACYT A1-S-033933 is gratefully acknowledged.

References

1 A. Kumar and P. Ghosh, *Eur. J. Inorg. Chem.*, 2012, 3955–3969.
2 H. Valdés, M. Poyatos, G. Ujaque and E. Peris, *Chem. – Eur. J.*, 2015, **21**, 1578–1588.
3 H. Valdés, M. Poyatos and E. Peris, *Inorg. Chem.*, 2015, **54**, 3654–3659.
4 E. Peris, *Chem. Rev.*, 2018, **118**, 9988–10031.
5 G. Le Duc, S. Meiries and S. P. Nolan, *Organometallics*, 2013, **32**, 7547–7551.
6 E. Rufino-Felipe, H. Valdés, J. M. Germán-Acacio, V. Reyes-Márquez and D. Morales-Morales, *J. Organomet. Chem.*, 2020, **921**, 121364.
7 S. P. Nolan, *N-Heterocyclic Carbenes: Effective Tools for Organometallic Synthesis*, Wiley, 2014.
8 S. Manzini, C. A. Urbina Blanco, D. J. Nelson, A. Poater, T. Lebl, S. Meiries, A. M. Z. Slawin, L. Falivene, L. Cavallo and S. P. Nolan, *J. Organomet. Chem.*, 2015, **780**, 43–48.
9 F. Shibahara, T. Mizuno, Y. Shibata and T. Murai, *Bull. Chem. Soc. Jpn.*, 2020, **93**, 332–337.
10 X. Yong, R. Thurston and C. Y. Ho, *Synthesis*, 2019, 2058–2080.
11 D. J. Nelson and S. P. Nolan, *Chem. Soc. Rev.*, 2013, **42**, 6723–6753.
12 H. V. Huynh, *Chem. Rev.*, 2018, **118**, 9457–9492.
13 H. V. Huynh, Y. Han, R. Jothibasu and J. A. Yang, *Organometallics*, 2009, **28**, 5395–5404.
14 A. Merschel, D. Rottschäfer, B. Neumann, H.-G. Stammler and R. S. Ghadwal, *Organometallics*, 2020, **39**, 1719–1729.
15 R. Dorta, E. D. Stevens, N. M. Scott, C. Costabile, L. Cavallo, C. D. Hoff and S. P. Nolan, *J. Am. Chem. Soc.*, 2005, **127**, 2485–2495.
16 T. Dröge and F. Glorius, *Angew. Chem., Int. Ed.*, 2010, **49**, 6940–6952.
17 R. A. Kelly Iii, H. Clavier, S. Giudice, N. M. Scott, E. D. Stevens, J. Bordner, I. Samardjiev, C. D. Hoff, L. Cavallo and S. P. Nolan, *Organometallics*, 2008, **27**, 202–210.
18 D. G. Gusev and E. Peris, *Dalton Trans.*, 2013, **42**, 7359–7364.
19 S. Díez-González and S. P. Nolan, *Coord. Chem. Rev.*, 2007, **251**, 874–883.
20 H. Jacobsen, A. Correa, A. Poater, C. Costabile and L. Cavallo, *Coord. Chem. Rev.*, 2009, **253**, 687–703.
21 A. Liske, K. Verlinden, H. Buhl, K. Schaper and C. Ganter, *Organometallics*, 2013, **32**, 5269–5272.
22 S. V. C. Vummaleti, D. J. Nelson, A. Poater, A. Gomez-Suarez, D. B. Cordes, A. M. Z. Slawin, S. P. Nolan and L. Cavallo, *Chem. Sci.*, 2015, **6**, 1895–1904.
23 Y. Koto, F. Shibahara and T. Murai, *Org. Biomol. Chem.*, 2017, **15**, 1810–1820.
24 M. S. S. Jamil and N. A. Endot, *Molecules*, 2020, **25**, 5161.
25 S. Byun, H. Seo, J.-H. Choi, J. Y. Ryu, J. Lee, W.-j Chung and S. Hong, *Organometallics*, 2019, **38**, 4121–4132.
26 E. Rufino-Felipe, R. Colorado-Peralta, V. Reyes-Márquez, H. Valdés and D. Morales-Morales, *Anti-Cancer Agents Med. Chem.*, 2021, **21**, 938–948.
27 C. Isanbor and D. O'Hagan, *J. Fluorine Chem.*, 2006, **127**, 303–319.
28 T. Ritter, M. W. Day and R. H. Grubbs, *J. Am. Chem. Soc.*, 2006, **128**, 11768–11769.
29 L. Á. Turcio-García, H. Valdés, S. Hernández-Ortega, D. Canseco-Gonzalez and D. Morales-Morales, *New J. Chem.*, 2022, **46**, 16789–16800.
30 J. M. Serrano-Becerra, S. Hernández-Ortega, D. Morales-Morales and J. Valdés-Martínez, *CrystEngComm*, 2009, **11**, 226–228.
31 D. A. Tomalia, *Nat. Mat.*, 2003, **2**, 711–712.
32 M. Rocha, G. A. Echeverría, O. E. Piro, J. L. Jios, S. E. Ulic and D. M. Gil, *J. Fluorine Chem.*, 2021, **242**, 109697.
33 C. Stein, R. Oswald, P. Sebald, P. Botschwina, H. Stoll and K. A. Peterson, *Mol. Phys.*, 2013, **111**, 2647–2652.
34 C. Dalvit, C. Invernizzi and A. Vulpetti, *Chem. – Eur. J.*, 2014, **20**, 11058–11068.
35 G. T. Giuffredi, V. Gouverneur and B. Bernet, *Angew. Chem., Int. Ed.*, 2013, **52**, 10524–10528.
36 S. Tsuzuki, T. Uchimaru and M. Mikami, *J. Phys. Chem. A*, 2006, **110**, 2027–2033.
37 J. T. Hutt and Z. D. Aron, *Org. Lett.*, 2011, **13**, 5256–5259.
38 A. Varadwaj, H. M. Marques and P. R. Varadwaj, *J. Comput. Chem.*, 2019, **40**, 1836–1860.
39 D. Chopra and T. N. G. Row, *CrystEngComm*, 2011, **13**, 2175–2186.
40 G. Cavallo, P. Metrangolo, R. Milani, T. Pilati, A. Priimagi, G. Resnati and G. Terraneo, *Chem. Rev.*, 2016, **116**, 2478–2601.
41 L. J. Barbour, *Compr. Supramol. Chem. II*, 2017, 23–43.
42 A. Parkin, G. Barr, W. Dong, C. J. Gilmore, D. Jayatilaka, J. J. McKinnon, M. A. Spackman and C. C. Wilson, *CrystEngComm*, 2007, **9**, 648–652.
43 P. R. Spackman, M. J. Turner, J. J. McKinnon, S. K. Wolff, D. J. Grimwood, D. Jayatilaka and M. A. Spackman, *J. Appl. Crystallogr.*, 2021, **54**, 1006–1011.